Proc. Natl. Acad. Sci. USA
Vol. 90, pp. 10469–10473, November 1993
Neurobiology

Relationship between intrinsic connections and functional architecture revealed by optical imaging and *in vivo* targeted biocytin injections in primate striate cortex

R. MALACH*, Y. AMIR, M. HAREL, AND A. GRINVALD

Department of Neurobiology, Weizmann Institute of Science, Rehovot 76100, Israel

Communicated by Ann M. Graybiel, July 2, 1993 (received for review May 13, 1993)

ABSTRACT **In primate primary visual cortex, neurons sharing similar response properties are clustered together forming functional domains that appear as a mosaic of patches or bands, often traversing the entire cortical depth from the pia to the white matter. Similarly, each cortical site connects laterally through an extensive network of intrinsic projections that are organized in multiple clusters (patches) and reach distances of up to a few millimeters. The relationship between the functional domains and these laterally connected patches has remained a controversial issue despite intensive research efforts. To investigate this relationship, we obtained high-resolution functional maps of the cortical architecture by *in vivo* optical imaging. Subsequently, extracellular injections of the sensitive anterograde tracer biocytin were targeted into selected functional domains. Within the ocular dominance system, we found that long-range intrinsic connections tended to link the monocular regions of same-eye ocular dominance columns. Furthermore, we discovered that binocular domains formed a separate set of connections in area V1; binocular regions were selectively connected among themselves but were not connected to strictly monocular regions, suggesting that they constitute a distinct columnar system. In the other subsystem subserving orientation preference, patches of intrinsic connections tended to link domains sharing similar orientation preferences. Analyses of the precision of these connections indicated that in both functional subsystems, <15% of the connections were between domains having orthogonal response properties. However, their selectivity was limited; ≈30% ± 10% of the interconnected patches contained neurons exhibiting orientation tuning that differed from those found at the injection sites by at least 45°. At short range (up to 400 μm from the injection site), this casual trend seemed markedly accentuated; the local, synaptic-rich axonal and dendritic arbors crossed freely through columns of diverse functional properties. These complex sets of connections can endow cortical neurons with a rich diversity of response properties and broad tuning.**

Ocular dominance and orientation columns are key elements in the functional architecture (1, 2) of striate cortex in cats and monkeys. The ocular dominance columns form a set of long bands running parallel to the cortical surface with interband distances of ≈400 μm. In contrast, it has been recently shown that orientation preference is organized according to a different principle; in upper cortical layers, domains activated by a single orientation appear as mosaic-like, circular or elliptical patches (3–7). The activity profile in response to a single orientation, across each patch, has a bell shape, with a diameter of ≈200 μm (half width at half height). Incremental changes in the orientation of the stimulus lead to a smooth shift in the positions of these domains. Patches of these orientation preference domains tend to form pinwheel-like structures (7–9). Here we refer to the orientation preference domains activated by a particular stimulus orientation as orientation domains.

Another set of functional domains in upper cortical layers is formed by clusters of cells that exhibit selective response properties to color and low spatial frequencies (10–12). These clusters contain high cytochrome oxidase (cyt_{ox}) activity and have been termed cyt_{ox} blobs. The cyt_{ox} blobs run precisely at the centers of ocular dominance columns (10). They interfere with, but do not grossly perturb, the architecture subserving orientation tuning (7, 11).

In parallel with these findings, neuroanatomical studies have revealed a conspicuous set of intrinsic horizontal connections linking neighboring cortical sites (11, 13–16). These intrinsic connections are most prominent in the upper cortical layers, extend to 2–3 mm in area V1 (17–19), and are thought to be excitatory (20, 21). A particularly striking feature of these connections is their tendency to arborize in preferred sites, forming distinct axonal clusters 200–300 μm in diameter (14, 17). Hereafter we use the term patches to refer to these axonal clusters.

Despite intensive research, the exact relationship between the axonal patches and the functional domains of ocular dominance and orientation preference remains controversial. Thus, it is not clear yet whether intrinsic connections in striate cortex are eye-dominance specific (22) or not (11) and whether domains of a particular orientation preference are selectively connected to each other (23) or to orthogonal orientation domains (24). The aim of this study was to answer the above questions and establish the degree of precision of intrinsic cortical connections at the level of a large population of neurons. A preliminary report was published in abstract form (25).

MATERIALS AND METHODS

Animals. Four anesthetized *Macaca fascicularis* adult monkeys were used in this study. The animals were anesthetized and their state was carefully monitored throughout the experiment. Detailed accounts of the procedures involved in the optical imaging and tract-tracing experiments have been described elsewhere (4, 7, 17, 26). Only a brief outline is given here.

Optical Imaging of Ocular Dominance and Orientation Domains. First, a selected cortical area was optically imaged while the animal received wide-field stimulation with square wave, black and white drifting gratings. Stimulation conditions included four to eight different orientations presented to either eye. Ocular dominance maps were obtained by dividing summed cortical images taken when the cortex was activated by stimulation of one eye by the other. Similarly,

The publication costs of this article were defrayed in part by page charge payment. This article must therefore be hereby marked "*advertisement*" in accordance with 18 U.S.C. §1734 solely to indicate this fact.

Abbreviation: cyt_{ox}, cytochrome oxidase.

*To whom reprint requests should be addressed.

orientation maps were obtained by dividing cortical images activated by orthogonal orientations (differential orientation maps) or by a vectorial addition (3) of several single condition (4, 8) orientation maps (angle or orientation preference maps; e.g., see Fig. 3*B*). The vectorial addition also provided information about the orientation tuning width at each cortical site (magnitude maps). Tests of the stability of the maps showed that for 80% of the pixels in the orientation maps, the rms deviation between two independent angle maps was only 7.5°. Large deviations were observed mostly around the pinwheel centers (7) and other small cortical regions exhibiting poor orientation tuning.

Biocytin Injections Targeted at Optically Identified Functional Domains. After the functional maps were obtained, cortical sites of interest received iontophoretic injections of the highly sensitive tracer biocytin (2% in Tris, pH 7.6; 4 μA/4 min, direct current). Ten injections were fully analyzed in relation to the optical maps. The tracer biocytin allows a precise definition of its effective tracer-uptake zone by localizing, under high magnification, labeled neuronal somata at the site of injection. Injection-site diameters varied from 100 to 300 μm. To avoid an overlap of biocytin patches corresponding to different injection sites, only one to four injections were placed in each mapped optical region. After the injections, animals were kept alive under anesthesia for another 8–12 hr with continuous monitoring of their physiological states and levels of anesthesia.

Histological Preparations. The animals were then sacrificed by pentobarbital overdose and perfused transcardially (phosphate-buffered saline followed by 2.5% glutaraldehyde/0.5% paraformaldehyde fix). The cortex was flattened (27) and cut tangentially at 60–80 μm. Alternate sections were stained for cyt_{ox} (28, 29) and biocytin. Sections were inspected and photographed under bright- and dark-field illumination (17).

Matching of Optical Maps with Histological Sections. To precisely match the optically derived maps with the histological sections, the pattern of superficial blood vessels was photographed during the recording session and then captured in the superficial histological sections. The two patterns were superimposed by using linear transformations of the entire images. Further refinement was gained by centering the cyt_{ox} blobs at the precise centers of all the ocular dominance bands imaged optically.

Computer-Assisted Demarcation of the Biocytin Patches. To determine the boundaries of the intrinsically connected patches, photomicrographs of the connectional patterns were digitized and filtered with a difference of gaussian operator ($s_2^2/s_1^2 = 3$). A boundary detection algorithm delineated the borders of the patches. Manual examination of all the biocytin patches analyzed for this report indicated that this procedure was efficient and objective (e.g., Fig. 1 *A* and *B*).

RESULTS

Lateral Connections Between Cortical Regions That Exhibit Monocular Responses. To evaluate the relationship between the laterally projecting axons and the system of ocular dominance columns, we first mapped the ocular dominance distribution optically and then targeted biocytin injections at the center of these columns. An example of such a case is shown in Fig. 1*A*. One can see by a casual examination that this injection site was connected to several distinct patches, beyond the "halo" of the injection. Fig. 1*B* shows the same injection with the patches formed outside the injection site halo outlined here by the automated procedure (see *Materials and Methods*). To explore the exact relationship of these biocytin patches to the ocular dominance columns we first superimposed the pattern of the biocytin patches on the cyt_{ox} blobs revealed in a neighboring section (Fig. 1*C*). Such

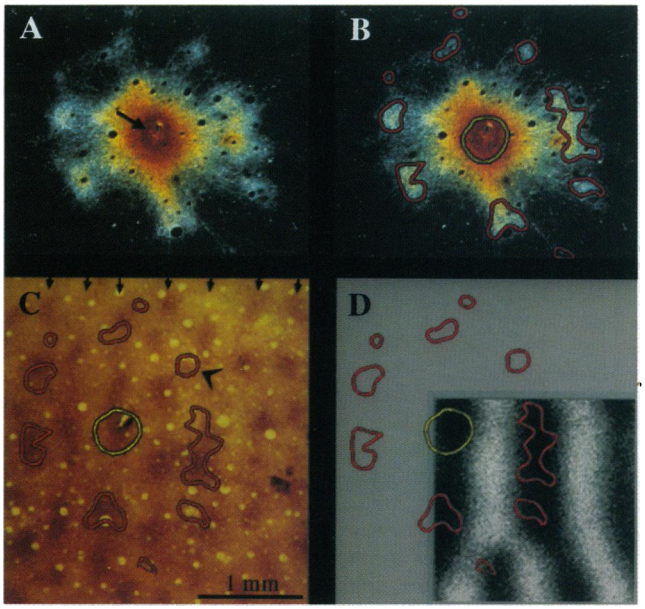

FIG. 1. Biocytin injection targeted at a monocular site in macaque monkey area V1. (*A*) Dark-field photomicrograph of a tangential cortical section showing a biocytin injection (arrow) that was targeted at the center of an ocular dominance column. Note extensive local halo around the injection site followed by clear axonal patches further away. (*B*) Same micrograph as in *A* but after the main patches were delineated (red contours; see *Materials and Methods*). The effective tracer-uptake zone, defined under high-magnification viewing (not shown), is depicted by the yellow contour. (*C*) A superimposition of the biocytin patches onto a neighboring cyt_{ox}-stained section. Note that the cyt_{ox} blobs form rows, which run top to bottom in the figure (indicated by small arrows). The biocytin patches tended to "skip" one row of cyt_{ox} blobs on each side of the injection. However, exceptions to this rule were found (e.g., arrowhead). (*D*) Same injection as in *C* but superimposed on an optically imaged map of ocular dominance columns. The injection was targeted at a contralateral eye column (coded black) at the top left corner of the optically imaged area. Note the tendency of the biocytin patches to skip over the ipsilateral eye column (coded white).

comparison is instructive since it has been established that rows of cyt_{ox} blobs are located at the centers of ocular dominance columns (10). The results showed that most of the patches "skipped" one row of cyt_{ox} blobs, suggesting that the majority of the long-range lateral connections were targeted at the same eye columns and avoided the opposite eye columns. However, there were also some clear violations of this rule—e.g., the patch indicated by an arrowhead, residing between the cyt_{ox} rows and therefore presumably in a more binocular region (Fig. 1*C*). Both the injection site and some of the patches overlapped cyt_{ox} blobs in apparent confirmation of the report that cyt_{ox} blobs are selectively interconnected (11). This indeed was the general impression from our data; however, we did not analyze this relationship quantitatively.

A more direct demonstration of the relationship between lateral connections and ocular dominance columns was obtained by using the optically derived functional map. Fig. 1*D* shows a superposition of these lateral connections on an optically derived ocular dominance map. The connections tended to cluster in the same eye column as that of the injection site and to skip the contralateral eye column. Such results were repeatedly observed for six injections targeted at, or close to, monocular sites.

Lateral Connections Between Binocular Regions. To test whether binocular regions are selectively interconnected, we targeted injections, in three cases, at binocular regions. Fig. 2*A* shows an example of such an injection superimposed on

an ocular dominance map. To demarcate the binocular regions more clearly, the same data of Fig. 2*A* are shown by using a gray scale (Fig. 2*B*) in which the cortical regions that exhibit equal responses to both eyes are coded black, while monocularly dominated sites are coded white. The patches of lateral connections clearly tended to reside in binocular regions, avoiding the highly monocular cortical regions. This was also reflected in the quantitative analysis (Fig. 2*C*), comparing the distribution of the degree of ocularity at the injection site (yellow bars) with that of the patchy projections (red bars). In this experiment, only 5% of the injected label spread into monocular regions (labeled right and left) and, similarly, only 10.5% of the patches overlapped with highly monocular regions. This finding suggests that the binocular regions contain a subsystem that has its own separate set of connections and is not merely a target for convergent projections from the two monocular ocular dominance columns.

To study how precise the lateral connections are in targeting sites of similar ocularity preference, a quantitative analysis was performed in which the eye preference of cortical neurons within the patches of lateral connections was compared to that found at the injection site. The results of this analysis, for three injections that were targeted at monocular cortical regions, are summarized in Fig. 2*D*. The histogram shows the distribution of pixel values in the optical map either at the injection site (yellow) or at the patches (red) as a function of ocularity; 87% of the pixels at the injection site had the same ocularity index as that of the center of the injection site. In contrast, the distribution within the patches was rather wide; only 65% of the pixels had the same ocularity index as that found at the center of the injection site. Despite this wider distribution, none of the patches linked regions dominated exclusively by the opposite eye, indicating that the lateral projections were far from random. Thus, the intrinsic lateral connections were quasi-specific with respect to ocularity.

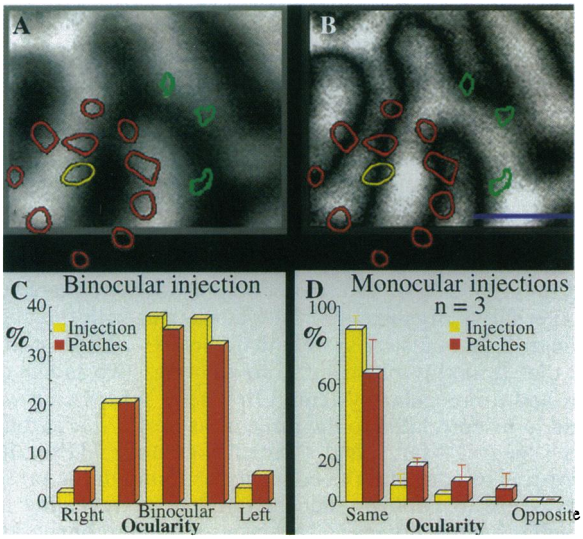

FIG. 2. Biocytin injection targeted at a binocular site. (*A*) A biocytin injection superimposed on a map of ocular dominance columns. The injection (yellow circle) was centered on a binocular zone. (*B*) Same injection and functional map, but here binocular zones are coded black, while monocular zones are coded in gray levels. The patches (red, dense; green, sparsely labeled) tended to avoid highly monocular sites and were located in binocular zones. (*C*) Quantitative analysis of the injection into a binocular site shown in *A* and *B*. Histogram shows the ocularity distributions at the injection site and the patches; horizontal axis shows the ocularity index that was divided into five levels. A minimal overlap of the patches with highly monocular zones was apparent. (*D*) Summary histogram showing the relationship between the ocular dominance preferences at the patches and at the injection sites for three injections centered on monocular sites.

Lateral Connections Among Orientation Domains. To examine the connectivity rules among orientation domains, we first obtained high-resolution optical maps of orientation preference (3, 4, 8, 30). An example of the labeling pattern of one injection, targeted at the center of an orientation domain, is shown in Fig. 3*A* superimposed on an orientation map. It is apparent that the majority of patches tended to be connected to orientation domains similar to that of the injection site. To quantify this relationship, the distributions of orientation preferences at the injection site and the patches were calculated as depicted by the two histograms shown in Fig. 3*B*. We found that at the injection site all of the neurons exhibited preferential responses to orientations of 180 ± 22.5, whereas at the patches only 66% had the same orientation tuning, indicating some level of divergence of connections to sites that exhibit different orientation preferences.

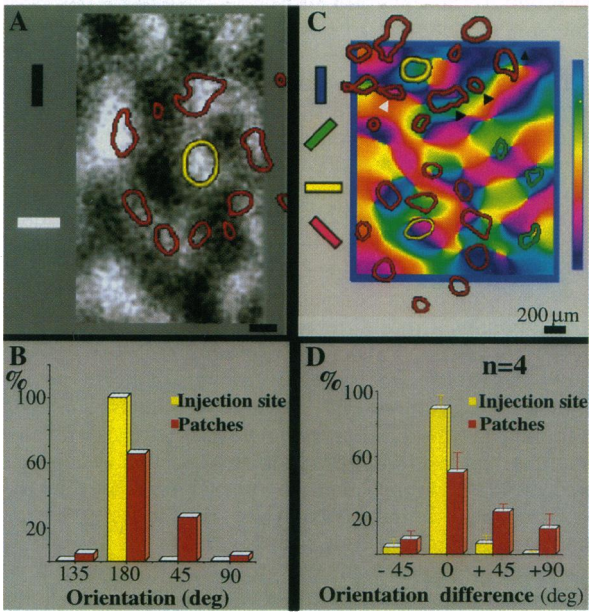

FIG. 3. Relationship of lateral connections to orientation domains. (*A*) Example of a biocytin injection targeted at an orientation domain responsive to horizontal stimulus orientation. Injection site and patches were superimposed on a differential map of horizontal (white) and vertical (black) orientation domains. Patches tended to overlap orientation domains of a similar orientation preference as that targeted by the injection. (*B*) A histogram of the case shown in *A*. The different orientations divided into four quadrants are shown on the horizontal axis. Yellow bar shows orientation preferences at injection sites. Red bars show distribution of orientation preferences in the connected patches. The patches targeted cortical regions of similar orientation preference as that of the injection site. However, the distribution of orientation preferences within the patches was considerably wider than that of the injection site. (*C*) Two injections superimposed on an orientation preference angle map (see *Materials and Methods*). Colors corresponding to four of the orientations are shown on the left, and the continuous color map used to code all orientations is shown on the right. The two injection sites (yellow) and their associated patches (red) were superimposed on this map. Certain patches (e.g., black arrowheads, top injection) possessed similar color combinations as this injection site, indicating matched orientation preferences, while other patches had different colors (e.g., white arrowhead). (*D*) Summary histogram of four cases with particularly localized injections (see text). Horizontal axis shows the difference in orientation preference at the center of the injection site and at the patches. The patch distribution peaked at 0°, indicating connections were to matched orientation domains. Once again, the distribution of orientation preference in the patches was substantially broader than that found within the cortical injection sites.

To obtain a more complete picture of the orientation specificity of connected patches, connectional patterns were superimposed on a high-resolution orientation-preference angle map obtained by optical imaging (Fig. 3*C*). In this color-coded functional map, each color shows the orientation preference at a given cortical site (3, 4, 8). Note that while some of the patches (black arrowheads) overlaid domains of the same orientation preference as that of the injection site (indicated by matched colors), others deviated from this rule (e.g., white arrowhead). An estimate of the difference in orientation preferences between the connected patches and the injection site is given in Fig. 3*D*. These histograms summarize results from four angle maps obtained for experiments in which the injection sites contained a narrow range of orientations. Similar to the single example shown in Fig. 3*C*, the histograms of the injection sites and patches peaked around the same orientation, indicating a tendency for matched orientation columns to be linked, but the distribution of orientation preferences at the patches was wider than that found at the injection sites.

Since angle maps show only the preferred orientation and disregard tuning width, we wondered whether the deviating patches were specifically targeting poorly tuned cortical regions. To examine this possibility, we repeated the analysis but excluded all the regions that were revealed by the magnitude maps to be poorly tuned. The results of this analysis were essentially the same (±1.5%) as before. Relating the labeling patterns of these injections to neighboring cyt_{ox}-stained sections revealed little, if any, overlap between these injection sites or the patches and the cyt_{ox} blobs. In summary, long-range connections link similar (<45°) orientation domains with a divergence of ≈30% ± 10%.

Anisotropy of the Patchy Connections. To test whether the overall distribution of labeled patches exhibited a radial symmetry, we filtered out the high spatial frequencies in photomicrographs of the connectional patterns. In all the injections, the resultant blurred image was clearly elliptical in shape, with its long axis running perpendicular to the direction of ocular dominance columns and the long/short axis ratio ranging from 1.4 to 2.2 (mean ± SD = 1.69 ± 0.211). This result provides a nice anatomical substratum for the anisotropy of the point spread image observed with voltage-sensitive dyes (A.G., unpublished work; ref. 31) near the V1/V2 border. Since next to the V1/V2 border the anisotropy of the magnification factor (32, 33) is similar to that reported here, it is likely that the overall shape of a family of patches was close to circular when projected onto visual space.

The Short-Range Connections. Inspection of all the injection sites revealed a massive network of local (i.e., less than ≈400 μm in diameter) axonal and dendritic arbors that form the halo emanating from the injection site. Such short connections carry numerous synaptic contacts uniformly distributed along their length and were explored in detail elsewhere (17). We repeatedly found that both dendritic arbors and local axonal connections tended to cross freely through boundaries of orientation and ocular dominance domains. Fig. 4 depicts two examples of such local connections and their relationship to the functional architecture. In Fig. 4*A*, images of the dendritic arbors of two upper layer neurons were superimposed on an orientation preference angle map taken from the same patch of cortex. Note the tendency of the dendrites to ignore the lines of curvature of the orientation maps and cross freely through regions of diverse orientation preference. A similar phenomenon can be observed in the axonal halo that formed around the injection site. In Fig. 4*B*, an image of the corresponding halo was superimposed on an orientation preference angle map. On closer examination, numerous individual fibers carrying synaptic boutons were followed from the site of injection, crossing a diverse set of orientations along their way.

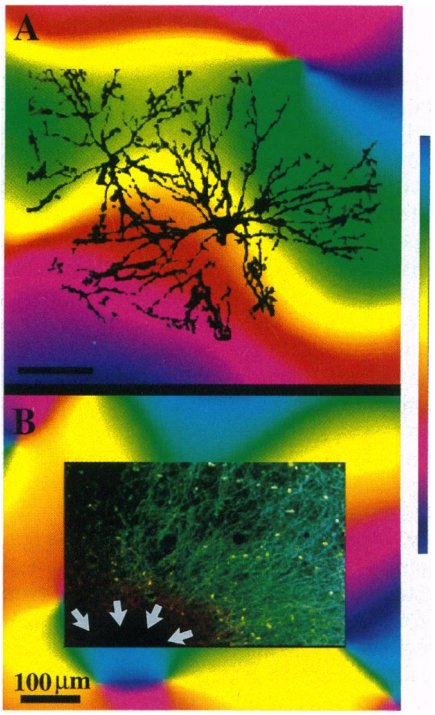

FIG. 4. Local connections and orientation domains. (*A*) Dendritic arbors of two upper layer neurons precisely superimposed on an orientation preference angle map taken from the same patch of cortex. (*B*) Enlarged view of local axonal plexus (halo) around the injection site superimposed on the orientation preference angle map. Arrows delineate effective tracer uptake zone as determined by high-power viewing. Injection was not centered on either an orientation center or a cyt_{ox} blob.

DISCUSSION

A Binocular Subsystem. It has been established (3, 4, 7, 34) that ocular dominance in upper cortical layers varies continuously from monocular regions for the right eye through binocular regions to monocular regions of the left eye, and so on. These results have suggested that the ocular dominance system is made up of two sets of columns: one for each eye. An alternative organization, fully consistent with the above findings, is an ocularity system that consists of at least three sets that smoothly blend into one another: two monocular ones and a binocular system (19). These subsystems were found to be correlated to the three classes of disparity tuned cells ["near," "far," and "tuned excitatory" (19)]. It is interesting to note that the connections found in the present study seem to confirm such distinction by revealing that binocular regions possess a separate set of interconnections. The present results, however, do not imply that these subsystems are discrete and sharply segregated from each other.

Specificity of Intrinsic Connections. Our results show a consistent trend in the relationship between intrinsic connections and the underlying functional architecture; functional domains sharing similar response properties tended to be connected to each other. In that respect, our results support the findings reported for orientation preference connectivity by Gilbert and Wiesel (15) in cat area 17 and argue against the claim (24) that orthogonal orientation domains are interconnected. Whether this discrepancy is related to different connectional rules exhibited by lateral connections in cat area 18 [the system Matsubara *et al.* (24) studied] and in monkey area 17 remains to be examined.

For the ocular dominance system, our results are in line with the suggestion, based on cross-correlation studies, that monkey ocular dominance columns of the same eye are interconnected (22). They are different from those of Singer and Lowel in the cat, which did not find eye-specific selectivity of connections in normally reared cats (35). However, they did find such selectivity in strabismic cats, raising the possibility that the more diffuse nature of ocular dominance organization in normal cat striate cortex, as compared to that of the macaque (34), may underlie this discrepancy.

The Precision of Long-Range Intrinsic Connections. Quantitative analysis of the data revealed that the targeting of functional domains by the lateral connections occasionally diverged to dissimilar functional domains. The achievement of functional precision in such a system may necessitate some sort of population coding that can "average" out the connectional deviations. Two preliminary reports relying on optical imaging and biocytin injections described similar observations in monkey and cat visual cortex (36, 37) and thus support the present conclusion. However, we do not rule out the alternative possibility that the "deviating patches" contain a subset of neurons, connected in a precise manner, to a different, undetermined, functional subsystem that partially overlaps the ocular dominance and orientation domains imaged here.

A Distributed Network of Short-Range Connections. Our results show that local axonal connections and dendritic arbors can cross freely through diverse functional domains. In a previous study, similar behavior was observed in the organization of dendritic arbors at the boundaries of cyt_{ox} blobs (29). At this stage, the mix of excitatory and inhibitor synapses in these local connections and their functional strength is not clear. A detailed study of synaptic distribution along such axons (17) has shown the existence of anatomical substrate for massive synaptic interactions in this region, which could provide a powerful route for cross talk and integration between neighboring, yet diverse, functional domains.

In conclusion, the observed balance between levels of specificity and diversity manifested by the horizontal connections vastly enlarges the potential repertoire of neuronal response properties while preserving the orderly organization at the level of entire neuronal populations. This anatomical architecture provides a suitable substrate for a range of functions such as fine grain interpolation (38), enhanced contrast sensitivity (19), plastic changes in cortical response properties (39–41), or construction of neuronal receptive fields within the primary visual cortex.

We thank Drs. E. Ahissar, S. Barash, D. Shoham, D. Malonek, and J. Olavarria for their helpful comments. This research was supported by a grant from the Israeli Academy of Arts and Sciences to R.M. and by Margaret Enoch, the Schilling, and the Green Foundations to A.G.

1. Mountcastle, V. B. (1957) *J. Neurophysiol.* **20,** 408–434.
2. Hubel, D. H. & Wiesel, T. N. (1968) *J. Physiol. (London)* **195,** 215–243.
3. Blasdel, G. G. & Salama, G. (1986) *Nature (London)* **321,** 579–585.
4. Ts'o, D. Y., Frostig, R. D., Lieke, E. E. & Grinvald, A. (1990) *Science* **249,** 417–420.
5. Swindale, N. V., Matsubara, J. A. & Cynader, M. S. (1987) *J. Neurosci.* **7,** 1414–1427.
6. Blasdel, G. G. (1992) *J. Neurosci.* **12,** 3139–3161.
7. Bartfeld, E. & Grinvald, A. (1992) *Proc. Natl. Acad. Sci. USA* **89,** 11905–11909.
8. Bonhoeffer, T. & Grinvald, A. (1991) *Nature (London)* **353,** 429–431.
9. Schwartz, E. L. & Rojer, A. (1992) *Soc. Neurosci. Abstr.* **313.11.**
10. Horton, J. C. & Hubel, D. H. (1981) *Nature (London)* **292,** 762–764.
11. Livingstone, M. S. & Hubel, D. H. (1984) *J. Neurosci.* **4,** 2830–2835.
12. Tootell, R. B. H., Silverman, M. S., Hamilton, S. L., De Valois, R. L. & Switkes, E. (1988) *J. Neurosci.* **8,** 1569–1593.
13. Rockland, K. S. & Lund, J. S. (1982) *Science* **215,** 1532–1534.
14. Rockland, K. S. & Lund, J. S. (1983) *J. Comp. Neurol.* **216,** 303–318.
15. Gilbert, C. D. & Wiesel, T. N. (1979) *Nature (London)* **280,** 120–125.
16. Gilbert, C. D. & Wiesel, T. N. (1983) *J. Neurosci.* **3,** 1116–1133.
17. Amir, Y., Harel, M. & Malach, R. (1993) *J. Comp. Neurol.* **334,** 19–46.
18. King, M. A., Lois, P. M., Hunter, B. E. & Walker, D. W. (1989) *Brain Res.* **497,** 361–367.
19. LeVay, S. (1988) *Prog. Brain Res.* **75,** 142–161.
20. McGuire, B. A., Hornung, J. P., Gilbert, C. D. & Wiesel, T. N. (1984) *J. Neurosci.* **4,** 3021–3033.
21. LeVay, S. (1988) *J. Comp. Neurol.* **269,** 265–274.
22. Ts'o, D. Y. & Gilbert, C. D. (1988) *J. Neurosci.* **8,** 1712–1727.
23. Gilbert, C. D. & Wiesel, T. N. (1989) *J. Neurosci.* **9,** 2432–2442.
24. Matsubara, J., Cynader, M., Swindale, N. V. & Stryker, M. P. (1985) *Proc. Natl. Acad. Sci. USA* **82,** 935–939.
25. Malach, R., Amir, Y., Bartfeld, E. & Grinvald, A. (1992) *Soc. Neurosci. Abstr.* **169.3.**
26. Frostig, R. D., Lieke, E., Ts'o, D. Y. & Grinvald, A. (1990) *Proc. Natl. Acad. Sci. USA* **87,** 6082–6086.
27. Tootell, R. B. & Silverman, M. S. (1985) *J. Neurosci. Methods* **15,** 177–190.
28. Wong-Riley, M. (1979) *Brain Res.* **171,** 11–28.
29. Malach, R. (1992) *J. Comp. Neurol.* **315,** 303–312.
30. Bonhoeffer, T. & Grinvald, A. (1993) *J. Neurosci.*, in press.
31. Grinvald, A., Bonhoeffer, T., Malonek, D., et al. (1991) in *Memory: Organization and Locus of Change*, eds. Squire, L. R., Weinberger, N. M., Lynch, G. & McGaugh, J. L. (Oxford Univ. Press, Oxford), pp. 49–85.
32. Van Essen, D. C., Newsome, W. T. & Maunsell, J. H. R. (1984) *Vision Res.* **24,** 429–448.
33. Hubel, D. H. & Wiesel, T. N. (1974) *J. Comp. Neurol.* **158,** 295–305.
34. Hubel, D. H. & Wiesel, T. N. (1968) *J. Physiol. (London)* **195,** 215–243.
35. Lowel, S. & Singer, W. (1992) *Science* **255,** 209–212.
36. Kisvarday, Z. F., Kim, D.-S., Eysel, U. T. & Bonhoeffer, T. (1992) *Soc. Neurosci. Abstr.* **169.2.**
37. Blasdel, G. G., Yoshioka, T., Levitt, J. B. & Lund, J. S. (1992) *Soc. Neurosci. Abstr.* **169.4.**
38. Barlow, H. B. (1980) *Proc. R. Soc. London B* **212,** 1–34.
39. Merzenich, M. M. & Kaas, J. H. (1982) *Trends Neurosci.* **5,** 434–436.
40. Gilbert, C. D. & Wiesel, T. N. (1992) *Nature (London)* **356,** 150–152.
41. Fiorani, M., Rosa, M. G. P., Gattas, R. & Rocha-Miranda, C. E. (1992) *Proc. Natl. Acad. Sci. USA* **89,** 8547–8551.